

# Optical absorption and band structure PbTe

T. R. Globus, B. L. Gel'mont, K. I. Geĭrman, V. A. Kondrashov, and A. V. Matveenko

(Submitted 13 August 1980)

Zh. Eksp. Teor. Fiz. 80, 1926–1939 (May 1981)

The optical characteristics of PbTe (the absorption spectrum  $\alpha(\hbar\omega)$ ) and the dispersion of the refractive index  $n(\hbar\omega)$  in the fundamental absorption region are obtained by measuring simultaneously, at  $T = 313$  K, the optical transmission and reflection of an epitaxial film on a BaF<sub>2</sub> substrate. The hole density at 77 K is  $\sim 10^{16}$  cm<sup>-3</sup>.  $\alpha(\hbar\omega)$  and  $n(\hbar\omega)$  are calculated by interference analysis with a computer. The width of the direct forbidden band at the point  $L$  is  $E_{gL} = 0.321$  eV. The longitudinal effective mass of the electrons and holes  $m_l = 0.195 m_0$  is close to the value determined from low-temperature experiments; this attests to the applicability of the Cohen model to the energy spectrum. Besides the principal band extrema, at the point  $L$  there are two additional extrema of the valence band in the direction of  $A$  ( $E_{gA} \approx 0.335$  eV) and in the  $A$  direction ( $E_{gA} \approx 0.41$  eV). The position of the maximum of the valence band at the point  $L$  relative to the remaining extrema changes position with change of temperature. The presence of an additional conduction-band extremum near the point  $W$ , separated from the minimum at the point  $L$  by an energy  $\sim 0.195$  eV is suggested. Steps and resonant peaks are observed against the background of the spectrum and are attributed to transitions, with phonon participation, between the levels of the states near the band extrema.

PACS numbers: 78.40.Ha, 78.20.Dj, 71.25.Tn

## 1. INTRODUCTION

The intrinsic absorption in PbTe at room temperature was investigated numerous times.<sup>1-5</sup> All the measurements yield close values of the width of the direct forbidden band,  $E_{gL} \approx 0.32$  eV, but the absorption coefficients obtained in different studies can differ by as much as a factor of two. In a number of cases, the experimental data were compared with the calculated dependence of the absorption coefficient  $\alpha$  on the radiation energy  $\hbar\omega$ .<sup>2,4,5,7</sup> The comparisons have shown that it suffices to take into account in the absorption spectrum the optical transitions between the closest band extrema at the point  $L$ , and that, at least up to energies  $\hbar\omega \approx (1.5-2)E_{gL}$ , if the parameters are suitably chosen the spectrum is well described both by the Kane model<sup>2,7</sup> and by more complicated models that take into account the interaction with the higher bands.<sup>4,6</sup> Thus, using a six-band model,<sup>4</sup> good agreement was obtained between the experimental data and with calculation, up to energies exceeding  $2E_{gL}$ .

It is well established by now, however, that PbTe has at least one additional series of valence-band extrema in the [110] direction (the point  $\Sigma$ ), separated from the fundamental extremum at low temperatures by  $\Delta E_{\Sigma} \approx 0.17$  eV (see Ref. 8 and the bibliography therein). It is also known that the gap between the valence subbands decreases with increasing temperature and that at room temperature both extrema are close in energy. From the data on the position of the edge of the optical absorption above room temperature,<sup>9</sup> and from an investigation of the temperature dependence of the kinetic coefficients,<sup>10</sup> it follows that the energy gap between the additional extremum  $V_{\Sigma}$  of the valence band and the minimum  $C_L$  of the conduction band is approximately constant at 0.34–0.38 eV.

Theoretical calculations of the band structure of PbTe by the pseudopotential method at low temperatures<sup>11-13</sup> point to the existence, besides the additional maximum  $V_{\Sigma}$  of the valence band in the [110] direction, also to the existence of a second additional maximum  $V_A$  inside the Brillouin zone, in the [111] direction; this

maximum is also sufficiently close in energy to the fundamental maximum at the point  $L$ , although this result has not been confirmed in other calculations.<sup>14</sup>

The existence of additional valence-band maxima close in energy to the fundamental one should lead to additional optical transitions and to a certain change in the character of the absorption spectrum near the corresponding energy thresholds. An investigation of the optical-absorption spectrum may be a direct method of confirming the complex band structure of PbTe, but this calls for exact experimental data obtained in a sufficiently wide energy range in the intrinsic-absorption region. At the same time, an exact determination of the absorption coefficient  $\alpha$  in a wide range from measurements of the optical transmission of thin samples is usually made complicated by the inevitable influence of interference effects that can introduce considerable errors in  $\alpha$ . It will be shown below that to obtain exact results it is necessary to measure simultaneously the transmission and reflection of one sample in the entire energy range of interest and to analyze the measurement results on the basis of interference formulas.

Our aim in the present paper was to obtain a maximum of exact data on the optical absorption of nondegenerate PbTe at room temperature. To this end, we measured the optical transmission  $T$  and reflection  $R$  of epitaxial films grown on a BaF<sub>2</sub> substrate at wavelengths 2–8  $\mu\text{m}$ . The optical parameters (the absorption coefficient  $\alpha$  and the refractive index  $n$ ) were determined by measuring  $T$  and  $R$  and using the technique of interference analysis with a computer, by a procedure described below.

## 2. MEASUREMENT AND CALCULATION OF THE OPTICAL PARAMETERS

The optical transmission was measured with an IKS-22A infrared spectrometer using a two-beam scheme, while the reflection was measured with an IKS-22A with a reflection-measurement attachment that ensured a near-normal ( $\sim 8^\circ$ ) angle of incidence on the sample.

The sample was illuminated from the film side (direct illumination) by an integral radiation flux, and the temperature was measured with a thermocouple. The results pertain to a temperature  $313 \pm 2$  K. The sample thickness  $d_2 = 0.61 \mu\text{m}$  was measured with an interference microscope accurate to  $\pm 1\%$ . The measurements of the transmission and reflection yielded typical interference patterns (see, e.g., Ref. 3). When the sample was mounted, particular attention was paid to avoidance of skewing. This was monitored against the coincidence of the extrema of  $T(\lambda)$  and  $R(\lambda)$  beyond the optical-absorption edge, in the region of small  $\alpha$  (the discrepancy did not exceed  $2-3 \text{ cm}^{-1}$ ). The room-temperature carrier density in the sample was close to the intrinsic value ( $p_{77} \approx 10^{16} \text{ cm}^{-3}$ ).

To calculate the absorption coefficient and the refractive index of a thin film on a transparent substrate we used the equations derived in Ref. 15 that connect the transmission and reflection of a film + substrate system with the film thickness and with the optical parameters of the film and of the substrate. In the case of direct illumination, the expressions for the transmission  $T_{13}$  and reflection  $R_{13}$  of the system, with allowance for multiple reflection in the substrate, are

$$T_{13} = \frac{(1-r_{12}^2)(1-r_{23}^2)e^{-\alpha_2 d_2}}{1+2r_{12}r_{23}e^{-\alpha_2 d_2} \cos 2\delta_2 + r_{12}^2 r_{23}^2 e^{-2\alpha_2 d_2}}, \quad (1)$$

$$R_{13} = \frac{r_{12}^2 + 2r_{12}r_{23}e^{-\alpha_2 d_2} \cos 2\delta_2 + r_{23}^2 e^{-2\alpha_2 d_2}}{1+2r_{12}r_{23}e^{-\alpha_2 d_2} \cos 2\delta_2 + r_{12}^2 r_{23}^2 e^{-2\alpha_2 d_2}}, \quad (2)$$

where  $r_{12}$  and  $r_{23}$  are the Fresnel coefficients on the air-film and film-substrate interfaces, respectively, and are equal to

$$r_{12} = \frac{n_1 - n_2}{n_1 + n_2}, \quad r_{23} = \frac{n_2 - n_3}{n_2 + n_3},$$

$n_1$ ,  $n_2$ , and  $n_3$  are the refractive indices of the air, film, and substrate,  $\alpha_2$  is the absorption coefficient of the film,  $d_2$  is the film thickness,  $\delta_2 = 2\pi n_2 d_2 / \lambda$  is the phase thickness of the film, and  $\lambda$  is the radiation wavelength. The expressions above are valid only in the case of relatively weak absorption by the film, when the relation  $n_2^2 \gg k_2^2$  is satisfied, where  $k_2 = \alpha_2 \lambda / 4\pi$  is the imaginary part of the complex refractive index of the film. In our case this condition is satisfied even at the largest  $\alpha_2$  ( $\lambda = 2 \mu\text{m}$ ,  $\alpha_2 \approx 3 \times 10^4 \text{ cm}^{-1}$ ,  $k_2 = 0.5$ ,  $n_2 = 5$ ).

For a bulky substrate, the measured values of the transmission  $T_{ex}$  and of the reflection  $R_{ex}$  of the system, with allowance for reflection from the second face of the substrate, are

$$T_{ex} = T_{13}(1-\bar{R}) / (1-\bar{R}R_{31}), \quad (3)$$

$$R_{ex} = R_{13} + \bar{R}T_{13}^2 / (1-\bar{R}R_{31}). \quad (4)$$

Here  $\bar{R} = (n_1 - n_3)^2 / (n_1 + n_3)^2$  is the coefficient of reflection from the air-substrate interface, and  $R_{31}$  is the coefficient of reflection of a substrate + film system, analogous to  $R_{13}$ , but for illumination from the substrate side. The quantity  $R_{31}$  in (3) and (4) amounts to only a small correction (since  $\bar{R} \approx 0.04$ ), and can be replaced with sufficient accuracy by the quantity  $R_{13}$  close to it.

The optical parameters  $\alpha$  and  $n$  of PbTe at the specified wavelength were determined with a computer by successive approximations. The described method of determining the optical parameters is very sensitive and can discern small changes of  $\alpha$  and  $n$  amounting to at least 1%. This, however, calls for satisfaction of special requirements with respect to the optical homogeneity of the sample and the accuracy with which  $T$ ,  $R$ , and  $d_2$  are measured. Otherwise it is impossible to obtain values of  $\alpha$  and  $n$  satisfying simultaneously both measured values of  $T$  and  $R$ . A check on the satisfaction of these requirements was made possible by performing the calculation in several steps. The positions of the  $\lambda_m$  extrema on the reflection curve  $R(\lambda)$  were first used to determine the values of the refractive index by the formula

$$n_2 = \lambda_m m / 4d_2, \quad (5)$$

where  $m$  is the order of the extremum. These values yielded an approximate relation for  $n_2(\lambda)$ . The preliminary values of  $n_2$  at the specified wavelength were used during the first stage of the calculation, in which values of  $\alpha_2(\lambda)$  satisfying Eqs. (1) and (3) were determined, and  $R_{ex}(\lambda)$  was calculated from Eqs. (2) and (4). The agreement between the calculated values  $R_{ex}$  and the experimental  $R$  in the extrema of the reflection, with accuracy  $(R_{ex} - R) \cdot 100 / R_{ex}$  not worse than 1% in the maxima  $dn$  not worse than 3% in the minima, indicates simultaneously that the sample is of good quality and the measurements were correctly performed. The final values of the optical parameters  $\alpha$  and  $n$  were determined during the last calculation stage by making small changes of the previously determined values of  $\alpha$  and  $n$  so as to fit both calculated values of  $T_{ex}$  and

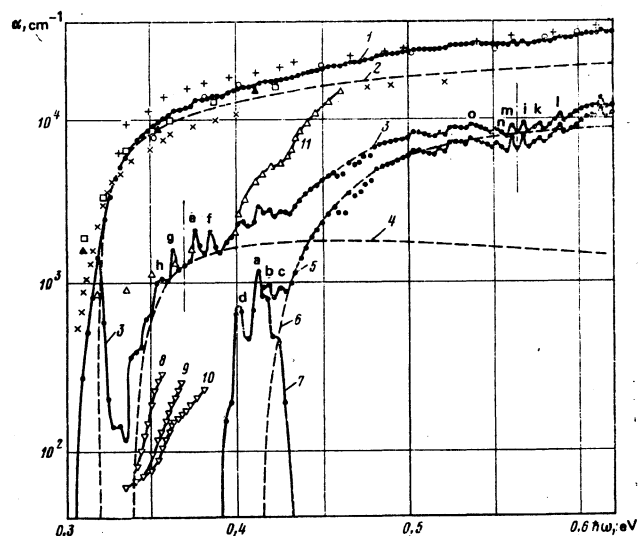


FIG. 1. Absorption coefficient  $\alpha$  vs. the radiation energy  $\hbar\omega$ . 1) Experimental plot of  $\alpha(\hbar\omega)$ ; 2) curve calculated in Cohen's model,  $\alpha_1(\hbar\omega)$ ; 3)  $(\alpha - \alpha_1)$ ; 4)  $\alpha_2(\hbar\omega)$ ; 5)  $(\alpha - \alpha_1 - \alpha_2)$ ; 6)  $\alpha_3(\hbar\omega)$ ; 7) impurity absorption near the threshold  $E_{G\alpha}$ . Experimental data from earlier studies: 8) 420 K, 9) 459 K, 10) 515 K from Ref. 9; 11)  $\Delta$ —685 K from Ref. 23;  $\times$ —Ref. 1,  $\circ$ —Ref. 2,  $\square$ —Ref. 3,  $+$ —Ref. 4,  $\blacktriangle$ —Ref. 5.

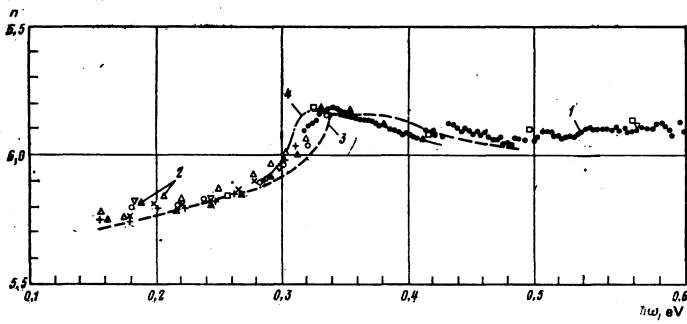


FIG. 2. Refractive index  $n$  vs. the radiation energy  $\hbar\omega$ . 1) Values of  $n$  from the data on  $R$  and  $T$ ; 2) values of  $n$  obtained from the positions of the extrema of  $R(\lambda)$ , 3) Ref. 17, 4) Ref. 3.

$R_{\text{ex}}$  to the measured ones. The calculations were made in wave-number steps of  $25 \text{ cm}^{-1}$ .

### 3. MEASURED OPTICAL CHARACTERISTICS AND THEIR ANALYSIS

Figures 1 and 2 show the results of the measurement of  $\alpha(\hbar\omega)$  and  $n(\hbar\omega)$  together with the results of some earlier work. Our values of  $\alpha$  (curve 1, Fig. 1) agree well with the data of Refs. 2 and 3 in the region of the fundamental absorption, and the differences do not exceed here 5%. Near the absorption edge our results have intermediate values and the difference from those of Ref. 3, where the measurements were made on  $p$ -type films with density  $1.5 \times 10^{18} \text{ cm}^{-3}$ , manifests itself in the absence of the "quasi-exponential tail." Scanlon's data<sup>1</sup> are substantially lower (the difference is approximately 40%) but, as shown in Ref. 16, where the optical characteristics of Pb were measured, Scanlon's data are lower there also by approximately 30%.

Figure 2 shows the values of the refractive index  $n$  in the intrinsic-absorption region, calculated from the measured  $R$  and  $T$ . It shows also the values of  $n$  obtained from the positions of the extrema of  $R(\lambda)$  for a number of  $n$ -type samples of varying thickness, principally beyond the intrinsic absorption edge. The value of  $n$  differs noticeably from the results of Refs. 3 and 17 only near the absorption edge. It is just in this region, however, that where at 1% uncertainty in the calculation of  $n$  leads to a 10% uncertainty in the value of  $\alpha$ .

We proceed now to analyze the results. It is well established by now that the optical absorption edge in PbTe at 300 K and lower temperatures is connected with direct allowed transition between the nearest band extrema at the point  $L$ . It is also known that in this case it is convenient to describe the dependence of the absorption coefficient on the energy  $\hbar\omega$  for a nondegenerate semiconductor in the coordinates  $(\alpha\hbar\omega)^2$  and  $\hbar\omega$ :

$$(\alpha\hbar\omega)^2 = A^2 E_{gL} (\hbar\omega - E_{gL}) K(z), \quad (6)$$

where  $A$  is a constant that can be determined from the initial linear section of the plot and is connected with the electronic parameters at the edges of the bands,  $E_{gL}$  is the width of the direct forbidden band, and  $K(z)$  is a correction function of  $z = \hbar\omega/E_{gL}$ , increases with increasing  $z$ , and has a form that depends on the band structure. We shall continue the analysis for two band-

structure variants usually employed for PbTe.<sup>18,19</sup> In Kane's two-band model variant, in which the longitudinal and transverse effective masses  $m_l$  and  $m_t$  are determined by the interaction of the nearest bands,<sup>2</sup> we have

$$A = \frac{4}{3} \frac{e^2 E_{gL}^{3/2}}{\hbar^2 c n} m_l^{1/2} m_t \left( \frac{1}{m_t} + \frac{2}{m_l} \right) \quad (7)$$

$$K(z) = \frac{(2z^2 + 1)^2 (z + 1)}{18z^2}. \quad (8)$$

In Cohen's model, in which only  $m_t$  is determined by the interaction of the nearest bands,

$$K(z) = \frac{1}{4z^2} \left\{ 1 + z^2 + (z-1) \left[ \frac{2}{3} + \frac{z-1}{5} \right] + \frac{2m_l}{m_t} (z-1)^2 \left[ \frac{z+1}{z} - \frac{2}{5} - \frac{z-1}{7} \right] \right\}^2, \quad (9)$$

(see the Appendix), the constant  $A$  contains only the longitudinal component of the effective mass

$$A = \frac{8}{3} \frac{e^2 E_{gL}^{3/2}}{\hbar^2 c n} m_l^{1/2}.$$

An attempt to determine exactly the parameters  $E_{gL}$  and  $A$  from a comparison of the experimental depen-

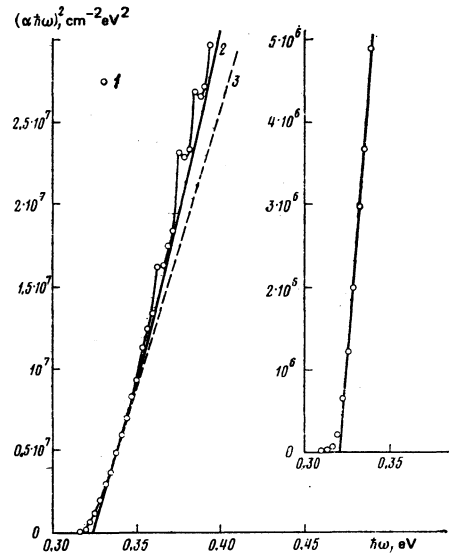


FIG. 3. Dependence of  $(\alpha\hbar\omega)^2$  on the radiation energy  $\hbar\omega$  near the threshold of direct transitions. 1) Experimental values, 2) calculated curve in Cohen's model, 3) extrapolation to a linear dependence on the initial section; inset—curves 2 and 3 coincide.

dence of  $(\alpha\hbar\omega)^2$  on  $(\hbar\omega)$  with the calculated curve encounters considerable difficulties. As seen from Fig. 3, even the initial section of the experimental plot is not straight because of the presence of the additional absorption, which is probably due to a contribution from indirect transitions or to impurities. On the other hand, at energies  $\hbar\omega > 0.35$  eV, the additional absorption already manifests itself in the form of repeated steps or even resonant peaks. The choice of the parameters  $E_{gL}$  and  $A$  is therefore not unique. Figure 3 shows an extrapolation to  $E_{gL} = 0.324$  eV, while the inset of Fig. 3 shows an initial section of the curve, for which extrapolation yields a value  $E_{gL} = 0.321$  eV. The limits of the possible values of the parameters  $E_{gL}$ ,  $A$ , and  $m_1/m_0$  ( $m_0$  is the mass of the free electron) as a function of the choice of the initial linear section are given in Table I. The band anisotropy coefficient  $m_1/m_1$  was assumed to be 5.5 at room temperature.

The parameters at the edge of the bands are not very sensitive to the choice of the model and, as seen from Table I, the obtained mean value of the longitudinal effective mass referred to the two bands is  $nl = 2/(m_{1c}^{-1} + m_{1v}^{-1}) = (0.195 \pm 0.035)m_0$ .

The published experimental values of the longitudinal effective mass in PbTe pertain to low temperatures and vary quite significantly. The best known values on the band edge, known from Ref. 20, are  $m_{1c} = 0.25m_0$  for the conduction band and  $m_{1v} = 0.31m_0$  for the valence band. In Ref. 19, analysis of all the known published data yielded, on the basis of the multiband model, most probable values  $m_{1c} = 0.15m_0$  and  $m_{1v} = 0.244m_0$ , which corresponds to a reduced value  $m_1 = 0.186m_0$  for the two bands. If the value  $m_1 = 0.195m_0$  obtained by us at room temperature is correct, then comparison with the data obtained at low temperatures does not confirm the growth of  $m_1$  with rising temperature, and hence with increasing  $E_{gL}$ . This fact cannot be explained within the framework of Kane's model and gives preference to Cohen's model. We nevertheless continued the analysis for both models and all the results that follow are in principle independent of the choice of the parameters within the domain of Table I, although Fig. 1 shows only one calculated curve 2 for  $\alpha_1(\hbar\omega)$ , obtained for the Cohen model at  $E_{gL} = 0.321$  eV.

The  $\alpha_1(\hbar\omega)$  curve corresponding to transition between nearest bands at the point  $L$ , lies at almost all energies below the general  $\alpha(\hbar\omega)$  curve, while curve 3 of Fig. 1, which represents the difference  $\alpha(\hbar\omega) - \alpha_1(\hbar\omega)$ , represents all the additional absorption. It is seen that the absolute value of the additional absorption is small and does not exceed 20–30% of the total absorption, with

TABLE I. Limiting values of the parameters  $E_{gL}$ ,  $A$ , and  $m_1/m_0$ .

$E_{gL}$ , eV	Kane's model		Cohen's model	
	$A$ , cm <sup>-1</sup>	$m_1/m_0$	$A$ , cm <sup>-1</sup>	$m_1/m_0$
0.321	$2.8 \cdot 10^4$	0.160	$2.9 \cdot 10^4$	0.195
0.324	$3.1 \cdot 10^4$	0.195	$3.2 \cdot 10^4$	0.230

the exception of the energy region near the fundamental absorption edge. Curve 3 of Fig. 1 is not uniform and can be relatively easily resolved into separate components. Foremost is the section near the absorption edge. It is most probable that this absorption is due to the participation of phonons. Favoring this assumption is the fact that this additional absorption is noticeable at energies lower than  $E_{gL}$  by an amount approximately equal to the energy of the longitudinal optical phonon, namely  $\sim 0.013$  eV for a phonon with a zero wave vector  $q$ .<sup>21</sup> In addition, just as in Refs. 1 and 9, the initial section of  $\alpha(\hbar\omega)$  can be represented as a straight line in the coordinates  $(\alpha\hbar\omega)^{1/2}$  and  $\hbar\omega$ . Nonetheless, without an additional investigation of the dependence of the absorption edge on the impurity density and on the temperature one cannot exclude the possibility of impurity absorption near  $E_{gL}$ .

The second additional-absorption region has a relatively distinct red boundary near  $\hbar\omega = 0.335$  eV. This section is characterized by the presence of a number of steps and peaks against the background of an increasing  $\alpha$ . The third additional-absorption region has an altered character of curve 3 and a new increase of  $(\alpha - \alpha_1)$  near the energy  $\hbar\omega \approx 0.41$  eV. The boundary of this region is masked by a number of peaks in the 0.4–0.43 eV range. Finally, at energies 0.5–0.6 eV one can see, on curve 3 of Fig. 1, a structure consisting of a number of peaks that are symmetrical about  $\hbar\omega = 0.564$  eV, followed by further increase of the additional absorption.

We proceed now to a more detailed analysis of the additional absorption, starting with the second region. For convenience in the second analysis, Fig. 4 shows the results of a theoretical calculation of the energy spectrum of PbTe at energies close to  $E_{gL}$ .<sup>11</sup> According to the calculation, the valence-bands have in the directions [110] and [111] extrema  $V_C$  and  $V_A$  separated by small energies from the extremum at the point  $L$ . The calculation results pertain to low temperatures and give tentative values of the gaps relative to the absolute minimum of the conduction band at the point  $L$ , vis.,  $E_{gC} \approx 0.33$  eV for  $V_C$  and  $E_{gA} \approx 0.4$  eV at the extremum  $V_A$  in the direction [111]. It follows also from Ref. 11 that the upper valence band at the point  $L$  is the most

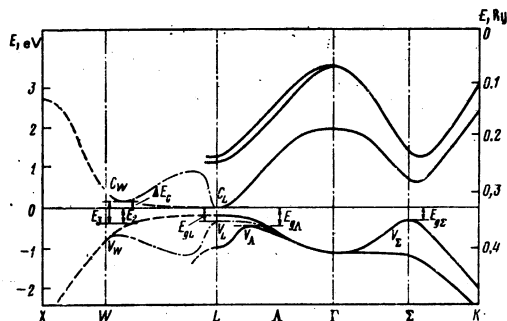


FIG. 4. Energy bands of PbTe near  $E_{gL}$ . Solid curves—calculations of Lin and Kleinman<sup>11</sup> ( $T = 0$  K); dash-dot curve—assumed form of the spectrum at room temperature in the  $L$ - $W$  direction.

sensitive to the change of the lattice potential. Consequently it is in fact this band which can change its position relative to the other bands, particularly when the temperature changes. At high temperatures, when the width of the direct forbidden band increases appreciably, the principal role should be assumed by indirect transitions from the lateral extrema  $V_C$  and  $V_A$  of the valence band, to the minimum of the conduction band. Indeed, from measurements of the temperature dependence of the optical absorption in the region  $\alpha < 300 \text{ cm}^{-1}$  (Ref. 9) it is known that the absorption edge at  $T > 400 \text{ K}$  does not depend on temperature and extrapolation of the dependence of  $\alpha^{1/2}$  on  $\hbar\omega$  yields a band gap  $\sim 0.33 \text{ eV}$  for indirect transitions. (These results are shown in part in Fig. 1, curves 8–10). The good agreement between the position of the additional-absorption edge obtained by us near  $\hbar\omega \approx 0.335 \text{ eV}$  with this value is obvious, and a comparison with the theoretical calculation data, with allowance for the fact that the position of the edge is independent of temperature, makes it possible to associate it with indirect transitions from the extremum  $V_C$  of the valence band to the minimum  $C_L$  of the conduction band.

The analysis of the form of the additional-absorption spectrum is made difficult by two circumstances. There are practically no data on the character of the equal-energy surfaces near the lateral extrema of the valence band. In addition, in our case the indirect transitions take place against a background of a continuous spectrum of allowed direct transitions. This casts doubts on the possibility of using the generally known expressions for the energy dependence of  $\alpha$  in the case of indirect transitions. It turned out nevertheless that the additional absorption in the energy band  $0.335\text{--}0.4 \text{ eV}$  is well approximated (disregarding the phonon structure) by the usual relation<sup>22</sup>

$$\alpha_2 \hbar\omega = B_2 (\hbar\omega - E_{g\Gamma} - \varepsilon_q)^2 / (\hbar\omega - E_{g\Gamma})^2, \quad (10)$$

where  $B_2$  is a constant, and  $\varepsilon_q$  is the phonon energy. Expression (10) pertains to the case of absorption with emission of one phonon, and the denominator of this expression is connected with the probability of intermediate vertical transitions. In our case this proba-

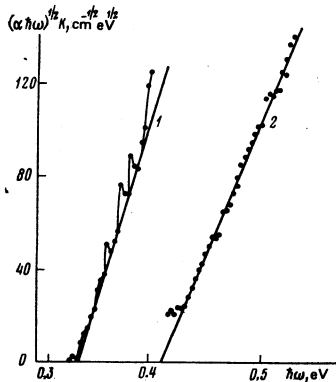


FIG. 5. Dependence of  $(\alpha \hbar\omega)^{1/2} K(\hbar\omega)$  on the radiation energy  $\hbar\omega$  near the threshold of the indirect transitions  $E_{g\Gamma}$  ( $\alpha_2$ ) and  $E_{gA}$  ( $\alpha_3$ ): 1)  $\alpha_2$ , 2)  $\alpha_3$ .

bility is high because the thresholds  $E_{g\Gamma}$  and  $E_{gA}$  of the direct and indirect transitions are close. Figure 5 shows the experimental data in accord with (10), plotted in coordinates  $(\alpha - \alpha_1)^{1/2} (\hbar\omega)^{1/2} K_2(\hbar\omega)$  and  $\hbar\omega$  (curve 1). The correction functions  $K_2(\hbar\omega) = (\hbar\omega - E_{g\Gamma}) / \Delta_2$  takes account here, in relative units ( $\Delta_2$  is an arbitrarily chosen energy difference,  $0.02 \text{ eV}$  in our case) the decrease of the transition probability with increasing distance from the threshold of the direct transitions. The lower envelope of the experimental points is a straight line that yields the threshold energy, including the phonon energy  $E_{g\Gamma} + \varepsilon_q = 0.337 \text{ eV}$ , and the constants  $B_2 = 1.0 \times 10^3 \text{ cm}^{-1} \text{ eV}$ . The  $\alpha_2(\hbar\omega)$  curve calculated from formula (10) is shown in Fig. 1 (curve 4). An indirect confirmation of the correctness of the analysis can be obtained by considering the temperature dependences given in Ref. 9 for the absorption connected with the indirect transitions, and by comparing the absorption spectra (curves 8–10 on Fig. 1) with  $\alpha_2(\hbar\omega)$ . It is seen that when the temperature is lowered, starting with  $515 \text{ K}$ , the intensity of the absorption near the threshold increases, although the position of the edge remains practically unchanged. The increase of  $\alpha$  is obviously connected with the fact that with decreasing temperature the value of  $E_{g\Gamma}$  decreases and comes closer to  $E_{gA}$ . At threshold values of  $\hbar\omega$ , the denominator in (19) is thus decreased and this effect is more substantial than the decrease of the coefficient  $B_2$ . The highest intensity of the indirect transitions near the threshold should be expected in the temperature region where  $E_{g\Gamma} \approx E_{gA}$ .

The absorption  $\alpha_2(\hbar\omega)$  is a relatively small part of the total additional absorption  $(\alpha - \alpha_1)$  in the energy region  $\hbar\omega > 0.4 \text{ eV}$ . This allows us to separate the next component of the additional absorption, by subtracting curve 4 from curve 3. The resultant plot of  $(\alpha - \alpha_1 - \alpha_2)$  is shown by curve 5 of Fig. 1. The possible errors in the extrapolation of  $\alpha_2(\hbar\omega)$  into the energy region  $\hbar\omega > 0.4 \text{ eV}$  have in practice little effect on the result. The threshold energy of this part of the additional absorption ( $\sim 0.4 \text{ eV}$ ) is close to the calculated energy  $E_{gA}$  of the indirect transitions between the extrema of the valence band  $V_A$  in the  $[111]$  direction and the extremum of the conduction band  $C_L$  at the point  $L$ . Just as the transitions from the extremum of the valence band  $V_C$ , optical transitions with a threshold  $E_{g\Gamma}$  should be observed at high temperatures, when  $E_{g\Gamma}$  becomes larger than  $E_{gA}$ . The experimental results of Ref. 23 confirm this assumption. The values of  $\alpha$  in that reference are shown for  $T = 685 \text{ K}$  in Fig. 1 (curve 11). The absorption coefficient increases appreciably starting with  $0.4 \text{ eV}$ , whereas the width of the direct forbidden band  $E_{g\Gamma}$  at this temperature is  $\sim 0.47 \text{ eV}$ .<sup>3</sup> Comparison with curve 3 points, in addition, to the absence of a noticeable temperature dependence of  $E_{gA}$ .

For indirect transitions one can expect in this case, too, the same energy dependence for  $\alpha$  as for  $\alpha_2$ . Therefore the experimental values of  $(\alpha - \alpha_1 - \alpha_2)$  are represented in Fig. 5 (curve 2) also in the coordinates  $(\alpha \hbar\omega)^{1/2} K_3(\hbar\omega)$  and  $\hbar\omega$ . The correction function in this case is  $K_3(\hbar\omega) = (\hbar\omega - E_{g\Gamma}) / \Delta_3$ , where  $\Delta_3$

$= 0.09$  eV. Except for the region near threshold, the experimental points fit a straight line well up to  $\hbar\omega \approx 0.5$  eV, and extrapolation yields a threshold energy  $E_{\text{FA}} + \varepsilon_q = 0.411$  eV and a constant  $B_3 = 1.15 \times 10^4$   $\text{cm}^{-1} \cdot \text{eV}$ . The curve calculated from (10) with these parameters values is shown in Fig. 1 (curve 6).

If PbTe has three valence-band extrema of close energy, of which one ( $V_L$ ) changes its position relative to the conduction band  $C_L$  with changing temperature, then  $p$ -type samples should show noticeable absorption in the IR region, due to transitions between different extrema of the valence band. The spectrum of this absorption can vary appreciably, depending on the temperature and doping. Such an absorption was indeed observed at room temperature in a number of studies,<sup>24-26</sup> starting with energies 0.07–0.1 eV. These threshold-energy values agree well with the difference  $\sim 0.09$  eV between the energies of the extrema  $V_L$  and  $V_A$ .

Curves 3 and 5 of Fig. 1, which represent the additional absorption, have pronounced individual resonance peaks as well as entire series of peaks whose positions are reliably reproducible (including the case when samples of different thickness are measured), although one cannot be certain of their shapes, owing to the insufficient resolution. One such series is seen on curve 5 near the 0.41 eV threshold and is apparently connected with  $E_{\text{FA}}$ . To our knowledge, there are no direct data on the state levels near the band edges in the case of PbTe. It is difficult, however, to find another explanation for the observed singularity, other than assuming that transitions with participation of phonons take place here between two discrete levels, one located near the maximum of the valence band  $V_A$ , and the other near the minimum of the conduction band  $C_L$ . These transitions can occur only with participation of phonons with wave vectors  $2\pi a^{-1}$  (0.15, 0.15, 0.15), where  $a$  is the lattice constant. The phonon spectrum for PbTe at room temperature is known<sup>21</sup> and the energies of the corresponding phonons are  $\varepsilon(\text{LO}) = 0.014$  eV and  $\varepsilon(\text{TO}) = 0.0045$  eV for longitudinal and transverse optical phonons and  $\varepsilon(\text{LA}) = 0.0045$  eV and  $\varepsilon(\text{TA}) = 0.0027$  eV for longitudinal and transverse acoustic phonons. Using these values, we can interpret the series of peaks near the 0.41 eV threshold (Fig. 1, curve 7) in the following manner: the energy of the transition between the levels near the extrema  $V_A$  and  $C_L$  is 0.409 eV, the peak "a" (0.4125 eV) is an unresolved double peak with emission of LA and TA acoustic phonons, the peaks "b" (0.4175) and "d" (0.401 eV) are the same with respective emission and absorption of a transverse optical TO phonon, and the peak "c" with emission of a longitudinal optical LO phonon.

The second series of phonon peaks has a very distinct symmetrical structure relative to the energy  $E_2 = 0.369$  eV. This energy is not connected in obvious fashion with any threshold energy whatever, so that it is impossible to identify unambiguously the transitions with which this structure is connected. It can be assumed, however, that transitions are observed in this

case between discrete levels separated by an energy 0.369 eV. The phonons that take part in the transitions are TO with energy 0.006 eV (peaks "g" and "e") and LO with energy 0.014 eV (peaks "h" and "f"). No participation of acoustic phonons is noticeable. We are unable to determine the directions of the transitions, but it appears that the transitions are indirect, since the energy of the transverse phonon that takes part in the transition is noticeably higher than the energy of TO with wave vector  $\mathbf{q} = 0$  ( $\sim 0.004$  eV).

The following series of phonon peaks, similar to some degree to the preceding one, is symmetrical about the energy  $E_3 = 0.564$  eV. Here, we assume, are observed transitions with absorption (peak "m") and with emission ("i") of a transverse optical phonon with energy  $\sim 0.004$  eV, and also with absorption and emission of one ("n" and "k") and two ("o" and "l") longitudinal optical phonons with energy  $\sim 0.013$  eV. These energy values correspond to phonons with zero vector  $\mathbf{q}$  and consequently indicate that the transitions are either direct or nearly direct. We assume that these two symmetrical series of peaks correspond to transitions from the same level to two different levels that are tied to two different band extrema and are separated by an energy  $\Delta E = E_3 - E_2 = 0.195$  eV. Since an almost continuous series of resonant peaks is observed starting with  $\sim 0.5$  eV, it is natural to assume that the additional extremum, which is separated by an energy  $\Delta E_c \approx 0.195$  eV, pertains to the conduction band, for in this case one can expect phonon structures at energies  $E_{\text{FL}} + \Delta E_c = 0.515$  eV,  $E_{\text{FL}} + \Delta E_c \approx 0.53$  eV, and  $E_{\text{FA}} + \Delta E_c \approx 0.604$  eV. Starting with these energy values, we can also expect further increase of the additional absorption, due to transitions from the three extrema of the valence band to the second minimum of the conduction band. As shown in Refs. 2 and 4, a noticeable excess of the absorption coefficient over the calculated value is indeed observed in this energy region. An experimental confirmation of the existence of an additional extremum of the conduction band can be the increase of the state density in the conduction band at an energy  $\sim 0.2$  eV deduced from the data on the thermoelectric power.<sup>18</sup> An attentive analysis of the data on optical absorption of  $n$ -PbTe beyond the edge of the fundamental band<sup>24,27</sup> also points to additional transitions at energies  $\hbar\omega \geq 0.2$  eV, although this absorption can be much smaller than the analogous absorption in  $p$ -PbTe of the same density.<sup>24</sup>

None of the theoretical calculations, to our knowledge, points directly to the existence of an additional conduction-band extremum separated by such a small gap from the fundamental one. Nonetheless, the results of Lin and Kleinman do make it possible to draw such a conclusion, since the calculation was not made for the  $L$ - $W$  and  $W$ - $X$  directions, but only at the points  $L$ ,  $W$ , and  $X$ . (This part of the spectrum is shown dashed in Fig. 4.) Recognizing that the  $L$ - $W$  direction is perpendicular to the  $[111]$  axis and that the effective mass at the point  $L$  is minimal in this direction, while the band curvature is maximal, a more probable energy spectrum is the one shown by the dash-dot line in Fig. 4. In this case extrema should exist near the

point  $W$  both in the conduction band ( $C_W$ ) and in the valence band ( $V_W$ ). Since, however, direct data confirming the existence of a second minimum of the conduction band are lacking at present, this assumption calls for verification in the future.

The location of the level with which the two symmetrical series of peaks are connected remains unclear. It can be assumed however, that it is connected with the extrema near the point  $W$ , as shown in Fig. 4. The reason is, as noted above, that the transitions near the energy  $E_3 = 0.565$  eV are close to direct.

#### 4. CONCLUSION

On the basis of the presently available data, our ideas concerning the energy spectrum of PbTe near  $E_{\epsilon L}$  reduce to the following.

At room temperature the edge of the optical absorption in PbTe is determined by direct allowed transitions between the fundamental band extrema at the point  $L$ , separated by an energy  $E_{\epsilon L} = 0.321$  eV ( $T = 313$  K). The energy spectrum near the point  $L$  corresponds more to the Cohen model than to the Kane model, i.e., the longitudinal effective mass  $m_l = 0.195m_0$  is determined not by the interaction of the nearest bands with each other, but by their interaction with the higher bands, since there is no noticeable increase of  $m_l$  with temperature, and hence with increasing  $E_{\epsilon L}$ .

Besides the extrema of the valence band at the points  $L$ , there are two additional series of extrema. The extremum in the  $\Sigma$ -[110] direction is close in energy to the maximum  $V_L$  at room temperature and is separated from the absolute minimum of the conduction band  $C_L$  by an energy  $E_{\epsilon L} \approx 0.335$  eV. The second series of additional extrema of the valence band is located, in accordance with the theoretical calculation, in the  $\Lambda$ -[111] direction and is separated from the conduction band by an energy  $E_{\epsilon \Lambda} \approx 0.41$  eV. With changing temperature, the extremum  $V_L$  of the valence band at the point  $L$  changes its energy position, relative to all the other extrema, whose mutual positions do not change noticeably. Above room temperature, with increasing  $E_{\epsilon L}$ , the optical-absorption edge begins to be governed by indirect transitions with energies  $E_{\epsilon \Sigma}$  and  $E_{\epsilon \Lambda}$ . The transitions from the extremum  $V_{\Lambda}$  are several times more intense than the transitions from the second indirect extremum  $V_{\Sigma}$ .

In the conduction band there is also an additional series of extrema, with preferred locations in the direction of the point  $W$  and separated from the absolute minimum at the point  $L$  by an energy gap  $\Delta E_c \approx 0.195$  eV.

Near all the band extrema there appear to exist levels of states that merge, within the limits of measurement accuracy, with the band edges. Since no special doping was carried out, these levels are possibly connected with intrinsic lattice defects, for example with deviations from stoichiometry. In addition to the levels near the band edges, there is apparently a deep level tied-in with the extremum near the point  $W$ , at an energy  $\sim 0.37$  eV lower than the absolute

minimum of the conduction band. The origin of this level is unknown.

Not all these foregoing results are equally reliable. We are convinced that the conclusions concerning the additional extrema of the valence band are correct. The assumption that the conduction band has an additional minimum must be verified. It is also possible that other explanations will be found for the observed absorption peaks which we attribute to the presence of discrete levels.

#### APPENDIX

The  $4 \times 4$  matrix of the Hamiltonian  $H(\mathbf{k})$ , which takes exact account of the interaction of the conduction band with the valence band at the point  $L$ , is given in Ref. 28.

In the case of unpolarized light, the imaginary part of the permittivity  $\kappa$  equals, in the random-phase approximation,

$$\text{Im } \kappa = -\frac{e^2 N}{12\pi(\hbar\omega)^2} \int d^3k \delta[E_c(\mathbf{k}) - E_v(\mathbf{k}) - \hbar\omega] \text{Sp}[H(\mathbf{k}) - E_c(\mathbf{k})] \sum_{\alpha=1}^3 \frac{\partial^2}{\partial k_{\alpha}^2} [H(\mathbf{k}) - E_v(\mathbf{k})], \quad (\text{A.1})$$

where  $E_c(\mathbf{k})$  and  $E_v(\mathbf{k})$  are the electron energies in the conduction band and in the valence band, respectively, and  $N$  is the number of ellipsoids. The transverse mass  $m_t$  of the electrons and holes, which is small compared with the longitudinal masses  $m_{lc}$  and  $m_{lv}$ , is determined mainly by the interaction of two bands—the upper valence band and the lower conduction band. At the same time, a substantial contribution can be made to the longitudinal mass by interactions with the remaining bands. We present here in explicit form the result for the case when the contribution of the other bands to the transverse masses can be neglected:

$$\text{Im } \kappa = \frac{Ne^2(\gamma m_l)^{1/2}}{3z\hbar(2E_{\epsilon L})^{1/2}} \left\{ 1 + \frac{1}{z^2} + \frac{\gamma}{3z^3} + \frac{\gamma^2\beta^2}{20z^2} - \frac{m_l}{2m_t} \left[ 2(\beta-1) + \frac{2}{3}\gamma \left( \frac{1}{z^2} - \beta^2 \right) + \frac{2\gamma^2\beta^2}{5z^2} + \frac{\gamma^4\beta^4}{14z^2} \right] \right\}. \quad (\text{A.2})$$

Here  $\beta = m_l(1/m_1^* + 1/m_{11}^-)/2$  characterizes the contribution of the remaining bands, other than the upper valence and lower conduction band, and the longitudinal masses of the electrons  $m_{lc}$  and of the holes  $m_{lv}$ :

$$\gamma = \frac{2}{\beta^2} \{ [1 + \beta^2(z^2 - 1)]^{1/2} - 1 \}.$$

The case of Kane's model ( $\beta = 0$ ) was considered in Ref. 18. The Cohen model ( $\beta = 1$ ,  $m_{lv} = m_1^*$ ,  $m_{lc} = m_1^-$ ) corresponds to the case when no contribution is made to the longitudinal masses by the interaction of the upper valence band with the lower conduction band.

<sup>1</sup>W. W. Scanlon, Phys. Rev. 8, 423 (1959) [sic].

<sup>2</sup>I. A. Drabkin, L. Ya. Morozovskii, I. V. Nel'son, and Yu. I. Ravich, Fiz. Tekh. Poluprov. 6, 1323 (1972) [Sov. Phys. Semicond. 6, 1156 (1972)].

- <sup>3</sup>N. Piccioli, J. M. Besson, and M. Balkanski, *J. Phys. Chem. Solids* **35**, 971 (1974).
- <sup>4</sup>O. Ziep and D. Genzow, *Phys. Stat. Sol. (b)* **96**, 359 (1979).
- <sup>5</sup>Yu. V. Mal'tsev, I. K. Smirnov, Yu. I. Ukhanov, and A. N. Veis, *J. de Physique* **29**, 99 (1968).
- <sup>6</sup>D. Genzow, A. G. Mironov, and O. Ziep, *Phys. Stat. Sol. (b)* **90**, 535 (1978).
- <sup>7</sup>I. A. Drabkin, Yu. Ya. Eliseeva, and I. V. Nel'son, *Fiz. Tekh. Poluprov.* **8**, 1382 (1974) [*Sov. Phys. Semicond.* **8**, 900 (1974)].
- <sup>8</sup>H. Sitter, K. Lischka, and H. Heinrick, *Phys. Rev.* **B16**, 680 (1977).
- <sup>9</sup>R. N. Tauber, A. A. Machonis, and I. B. Cadoff, *J. Appl. Phys.* **37**, 4855 (1966).
- <sup>10</sup>A. A. Andreev, *J. de Physique* **29**, 50 (1968).
- <sup>11</sup>P. J. Lin and L. Kleinman, *Phys. Rev.* **142**, 478 (1966).
- <sup>12</sup>R. L. Bernick and L. Kleinman, *Solid State Commun.* **8**, 569 (1970).
- <sup>13</sup>P. J. Lin, W. Saslov, and M. L. Cohen, *Solid State Commun.* **5**, 893 (1967).
- <sup>14</sup>M. L. Cohen, Y. Tung, and Ph. B. Allen, *J. de Physique*, **29**, C-4, 164 (1968); Y. Tung and M. L. Cohen, *Phys. Rev.* **180**, 823 (1969).
- <sup>15</sup>V. E. Kondrashov, *Optika fotokatodov (Optics of Photocathodes)*, Nauka, 1976, p. 17.
- <sup>16</sup>R. B. Schoolar and J. R. Dixon, *Phys. Rev.* **137**, 667 (1965).
- <sup>17</sup>J. N. Zemel, J. D. Jensen, and R. B. Schoolar, *Phys. Rev.* **140**, A330 (1965).
- <sup>18</sup>I. N. Dubovskaya and Yu. I. Ravich, *Fiz. Tverd. Tela (Leningrad)* **8**, 1455 (1966) [*Sov. Phys. Solid State* **8**, 1160 (1966)].
- <sup>19</sup>G. M. T. Foley and D. N. Langenberg, *Phys. Rev.* **B15**, 4850 (1977).
- <sup>20</sup>K. F. Cuff, M. R. Ellett, C. D. Kuglin, L. R. Williams, *Intern. Conf. Physics of Semiconductors, Paris, 1964*, p. 677.
- <sup>21</sup>W. Cochran, R. A. Cowley, G. Dolleng, and M. M. Elcombe, *Proc. Roy. Soc. A*-**293**, 433 (1966).
- <sup>22</sup>T. S. Moss, G. J. Burrell, and B. Ellis, *Semiconductor Opto-Electronics*, Butterworths, 1973. Russ. transl. Mir, 1976, p. 72.
- <sup>23</sup>A. N. Veis, V. I. Kaidanov, Yu. I. Ravich, I. A. Ryabtseva, and Yu. I. Ukhanov, *Fiz. Tekh. Poluprov.* **10**, 104 (1976) [*Sov. Phys. Semicond.* **10**, 62 (1976)].
- <sup>24</sup>H. R. Riedl, *Phys. Rev.* **127**, 162 (1962).
- <sup>25</sup>A. N. Veis and Yu. I. Ukhanov, *Fiz. Tekh. Poluprov.* **10**, 1315 (1976) [*Sov. Phys. Semicond.* **10**, 780 (1976)].
- <sup>26</sup>B. F. Gruzinov, I. A. Drabkin, Yu. Ya. Eliseeva, E. Ya. Lev, and I. V. Nel'son, *ibid.* **13**, 1308 (1979) [**13**, 767 (1979)].
- <sup>27</sup>I. K. Smirnov and Yu. I. Ukhanov, *ibid.* **5**, 1103 (1971) [**5**, 971 (1971)].
- <sup>28</sup>J. O. Dimmock, *Physics of Semimetals and Narrow-Gap Semiconductors. Proc. of Conference, Dallas, Texas, 1970*, p. 319.

Translated by J. G. Adashko